The EMBO Journal Vol. 21 No. 14 pp. 3829–3840, 2002

Class I tyrosyl-tRNA synthetase has a class II mode of cognate tRNA recognition

Anna Yaremchuk[1,2], Ivan Kriklivyi[2], Michael Tukalo[1,2,3] and Stephen Cusack[1,3]

[1]European Molecular Biology Laboratory, Grenoble Outstation, c/o ILL, 156X, F-38042 Grenoble cedex 9, France and [2]Institute of Molecular Biology and Genetics, NAS of Ukraine, 252627 Kiev-143, Ukraine

[3]Corresponding authors
e-mail: cusack@embl-grenoble.fr or tukalo@embl-grenoble.fr

Bacterial tyrosyl-tRNA synthetases (TyrRS) possess a flexibly linked C-terminal domain of ~80 residues, which has hitherto been disordered in crystal structures of the enzyme. We have determined the structure of *Thermus thermophilus* TyrRS at 2.0 Å resolution in a crystal form in which the C-terminal domain is ordered, and confirm that the fold is similar to part of the C-terminal domain of ribosomal protein S4. We have also determined the structure at 2.9 Å resolution of the complex of *T.thermophilus* TyrRS with cognate tRNA^{tyr}(GΨA). In this structure, the C-terminal domain binds between the characteristic long variable arm of the tRNA and the anti-codon stem, thus recognizing the unique shape of the tRNA. The anticodon bases have a novel conformation with A-36 stacked on G-34, and both G-34 and Ψ-35 are base-specifically recognized. The tRNA binds across the two subunits of the dimeric enzyme and, remarkably, the mode of recognition of the class I TyrRS for its cognate tRNA resembles that of a class II synthetase in being from the major groove side of the acceptor stem.

Keywords: class I aminoacyl-tRNA synthetase/ribosomal protein S4/tRNA recognition/tyrosyl-tRNA synthetase/ X-ray crystallography

Introduction

Tyrosyl-tRNA synthetase (TyrRS) is a class I aminoacyl-tRNA synthetase, but is unusual in that it is a functional dimer, a feature only shared with tryptophanyl-tRNA synthetase amongst class I synthetases (Cusack, 1995). It was the first synthetase to have its crystal structure solved (Bhat *et al*., 1982), including its substrate complexes with tyrosine and tyrosyl-adenylate (Brick and Blow, 1987; Brick *et al*., 1989), and both the mechanism of tyrosyl-adenylate formation (reviewed in Fersht, 1987; First, 1997) and its interaction with cognate tRNA^{tyr} (reviewed in Bedouelle, 1990; Bedouelle *et al*., 1993) have been the subject of intense biochemical study. However, there remain a number of significant areas where structural data that correlate with biochemical observations are lacking. Here we report the first crystal structure of a bacterial tyrosyl-tRNA synthetase complexed with cognate tRNA^{tyr}. This permits us to visualize the mode of interaction of this synthetase for its cognate tRNA, which in prokaryotes, but not archaea or eukaryotes, is of the class 2 type, i.e. with a long variable arm. The enzyme subunit comprises an N-terminal Rossmann-fold catalytic domain, characteristic of class I synthetases, followed by a central α-helical domain and, finally, a putative tRNA-binding C-terminal domain of ~80 residues, which has been invisible until now due to disorder in all crystal structures of TyrRS (Brick *et al*., 1989; Qiu *et al*., 2001). The structure described here reveals the exact role in specific tRNA recognition of the flexibly linked C-terminal domain and also shows how unique tertiary interactions in the core of tRNA^{tyr} lead to a different orientation of the long variable arm, permitting discrimination from other long variable arm (class 2) tRNAs such as tRNA^{ser}. The structure confirms the expected cross-subunit binding of the tRNA (Bedouelle, 1990). Furthermore, the mode of recognition of TyrRS for its cognate tRNA is similar to that of a class II synthetase rather than a canonical class I synthetase (Rould *et al*., 1989; Ruff *et al*., 1991), a significant evolutionary anomaly.

Results and discussion

We have cloned and overexpressed TyrRS from the hyperthermophilic eubacterium *Thermus thermophilus* (TyrRSTT; strain HB27). It has a subunit of 432 residues and shares a branch in the phylogenetic tree of eubacterial TyrRS with the enzymes from *Deinococcus radiodurans*, *Aquifex aeolicus*, *Haemophilus influenzae* and *Helicobacter pylori*, distinct from the branch containing *Bacillus stearothermophilus*, *Escherichia coli* and eukaryotic mitochondrial TyrRS, for example (Wolf *et al*., 1999). Non-bacterial TyrRS, which recognize class I tRNAs without a long variable arm, are quite distinct and either lack (archaeal) or have an alternative (eukaryotic) C-terminal domain (Steer and Schimmel, 1999). This evolutionary divergence correlates with a systematically different first base pair of the cognate tRNA^{tyr} acceptor stem, G1–C72 in prokaryotes and mitochondria, and C1–G72 in eukaryotes and archaea. This difference means that there is no cross-charging between eukaryote and prokaryote synthetases and tRNA^{tyr}s, (e.g. Quinn *et al*., 1995). The sequence identity between TyrRSTT and *B.stearothermophilus* TyrRS (TyrRSBSt), whose atomic structure is known (Brick *et al*., 1989), is relatively low (28%; Figure 1) and the relative orientation of the domains is sufficiently different that the structure of TyrRSTT had to be solved *de novo* using the single isomorphous replacement with anomalous scattering (SIRAS) method (our unpublished results).

We have also determined a series of structures of TyrRSTT complexed with various combinations of ATP

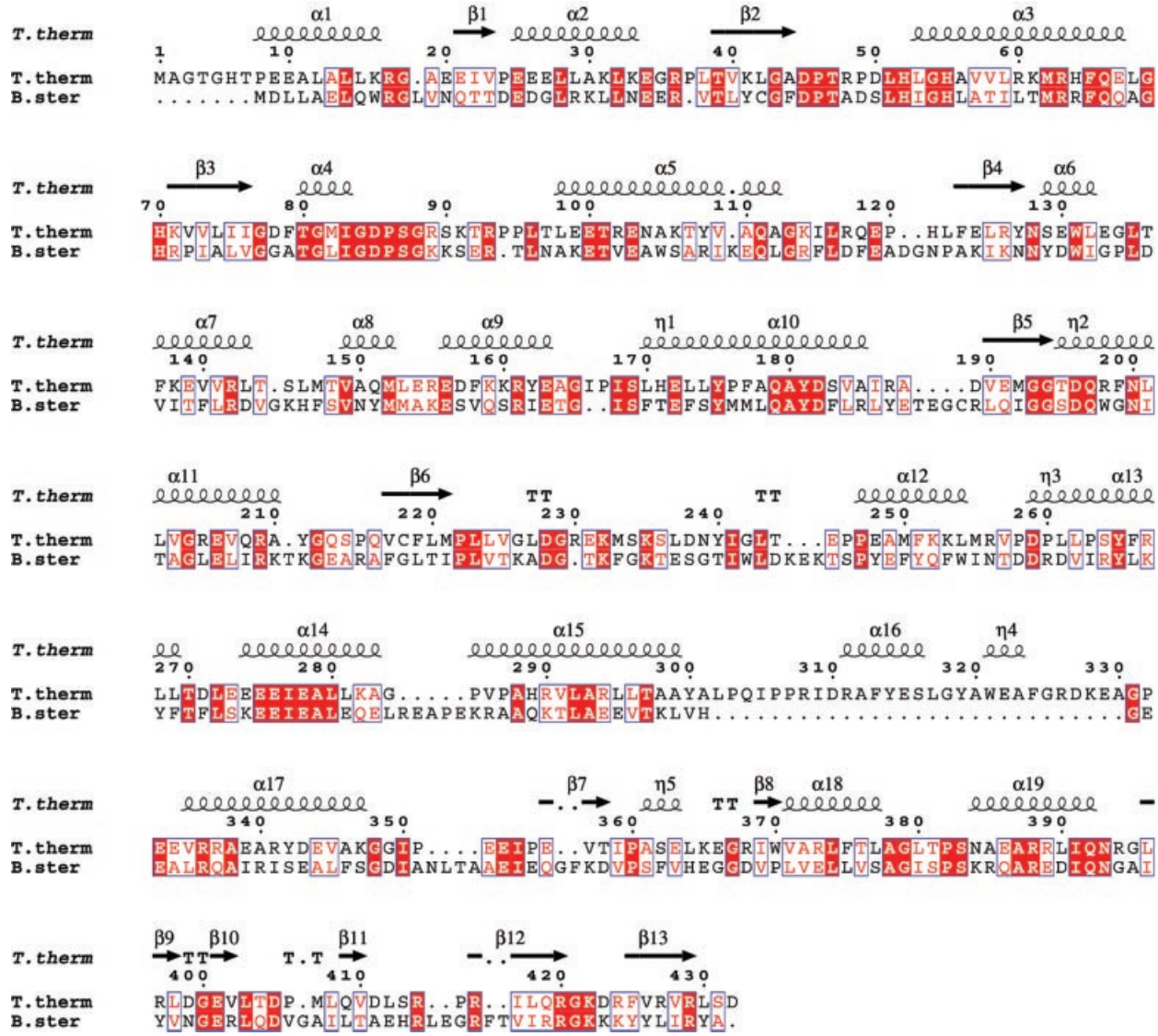

Fig. 1. Structure-based sequence alignment of tyrosyl-tRNA synthetase from *T.thermophilus* and *B.stearothermophilus*. The secondary structure of the TyrRSTT structure, calculated using DSSP (Kabsch and Sander, 1983), is superposed on top. Note the TyrRSTT-specific insertion between residues 302 and 330. The figure was prepared using ESPript (Gouet *et al.*, 1999).

and tyrosine, which address several questions relating to the mechanism of tyrosine activation. A full description of these results is beyond the scope of this paper; however, we can summarize the results in the following points. We observe that the TyrRSTT active site domain has a very plastic structure, which is remodelled, to a greater or lesser extent, at the level of side-chain orientations, backbone conformations and interdomain orientations, depending on which combination of substrates is bound (e.g. no substrates, tyrosine only, ATP only, ATP and the non-reactive analogue tyrosinol or tyrosyl-adenylate). The apo-enzyme has an open active site with a poorly ordered flexible loop (residues 80–100), and the catalytically important 51-HIGH and 233-KMSKS motifs are withdrawn from the active centre. In contrast, the ternary complex with ATP and the non-reactive tyrosine analogue tyrosinol is the most closed state, with all regions fully ordered and the KMSKS loop fully engaged with the ATP. Binding of tyrosine or tyrosinol alone only partially orders the active site (see below and Figure 2A). Binding of ATP or adenylate, in addition to ordering the KMSKS loop, also leads to a slight change in the relative orientation of the Rossmann-fold catalytic domain and the α-helical domain.

Crystal structure of T.thermophilus tyrosyl-tRNA synthetase including the C-terminal domain

One particular crystal form of TyrRSTT, co-crystallized with tyrosinol, and in which the dimer is the asymmetric unit (Table I), allows visualization for the first time of the complete enzyme including the C-terminal domain at 2.0 Å resolution. This domain (residues 352–432 in TyrRSTT) is connected to the preceding α-helical domain by a completely flexible peptide (residues 345–351), which is only partially visible in the structure. As a result, in the absence of bound tRNA, the two C-terminal domains of the dimer are observed in quite different orientations, as determined by crystal packing (Figure 2A). In a related crystal form,

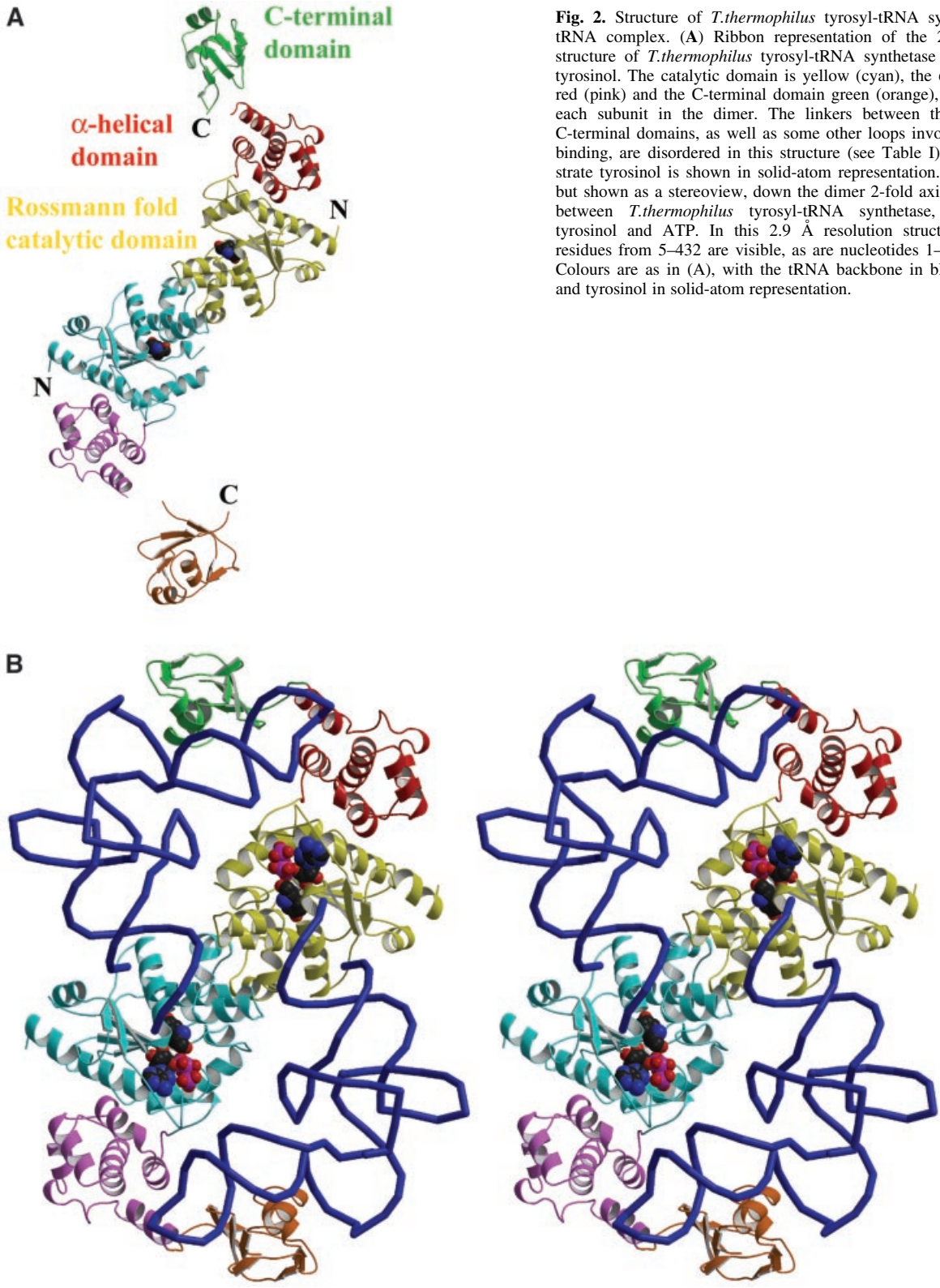

Fig. 2. Structure of *T.thermophilus* tyrosyl-tRNA synthetase and its tRNA complex. (**A**) Ribbon representation of the 2.0 Å resolution structure of *T.thermophilus* tyrosyl-tRNA synthetase complexed with tyrosinol. The catalytic domain is yellow (cyan), the α-helical domain red (pink) and the C-terminal domain green (orange), respectively, for each subunit in the dimer. The linkers between the α-helical and C-terminal domains, as well as some other loops involved in substrate binding, are disordered in this structure (see Table I). The small substrate tyrosinol is shown in solid-atom representation. (**B**) Same view, but shown as a stereoview, down the dimer 2-fold axis of the complex between *T.thermophilus* tyrosyl-tRNA synthetase, tRNA^{tyr}(GΨA), tyrosinol and ATP. In this 2.9 Å resolution structure, all enzyme residues from 5–432 are visible, as are nucleotides 1–74 of the tRNA. Colours are as in (A), with the tRNA backbone in blue and the ATP and tyrosinol in solid-atom representation.

but obtained in the absence of any substrate, only one C-terminal domain is ordered (data not shown). In a third different crystal form, in which the monomer is the asymmetric unit, the C-terminal domain is invisible, as was the case for the TyrRS from *B.stearothermophilus* (Brick *et al*., 1989) and *Staphylococcus aureus* (Qiu *et al*., 2001). These observations are in agreement with conclusions from studies of the isolated C-terminal domain (Guez *et al*., 2000). Note that in the structure of TyrRSTT co-crystallized with tyrosinol, the presence of the tyrosinol substrate is not sufficient to fully order the active site. In particular, the loop 80–100 is poorly visible and other

Table I. Data collection and refinement statistics for TyrRSTT structures

Crystal	TyrRSTT + tyrosinol	TyrRSTT-tRNA^{tyr}(GΨA) + tyrosinol + ATP
Beamline/detector	ID14-EH1, MarCCD	ID14-EH4, ADSC Quantum 4
Wavelength	0.934 Å	0.939 Å
Exposure/image	18 s/1°	4 s/0.5°
Space group	$P2_12_12_1$	$P3_121$
Cell dimensions (Å)	a = 67.8, b = 111.1, c = 141.2	a = 129.5, b = 129.5, c = 109.5, γ = 120
Resolution	25–2.0 Å	23–2.9 Å
Total reflections	464 280	76 961
Unique reflections	70 951	22 669
Average redundancy (highest bin)	6.5 (2.4)	3.4 (1.8)
Completeness (%) (highest bin)	97.6 (84.5)	94.9 (63.8)
R-merge (highest bin)	0.089 (0.306)	0.075 (0.509)
Refinement		
Resolution (Å)	20–2.0	20–2.9
Solvent content (%)	56	70
Work reflections	67 348	21 473
Test reflections	3557 (4.9%)	1146 (4.8%)
R-free/R-work	0.260/0.233	0.271/0.221
Contents of asymmetric unit	TyrRSTT dimer (chains A/B), each monomer with bound tyrosinol	TyrRSTT monomer with one tRNA, ATP and tyrosinol
No. of protein atoms in model	3231 (A) + 3256 (B)	3403
Poorly ordered regions	A: 1–4, 80–100, 348–351 B: 1–4, 84–96, 345–352	Nucleotides 74–76. Bases of . nucleotides 16, 20, 474
No. of tRNA atoms	–	1753
No. of solvent molecules	254 water, 5 sulfate	13 water
No. of substrate atoms	24 (2× tyrosinol)	31 (ATP), 12 (tyrosinol)
<b> protein (Å^2)	31.3	65.3
<b> tRNA (Å^2)	-	88.8
<b> solvent (Å^2)	34.4	47.2
<b> substrate (Å^2)	38.2	56.5
Anisotropic B-factor correction (Å^2)	B11 = 4.06, B22 = –8.77 B33 = 4.72, B12 = 0.0 B13 = B23 = 0.0	B11 = B22 = –10.0 B33 = 20.0, B12 = –24.5 B13 = B23 = 0.0
R.m.s.d. bonds (Å)	0.006	0.008
R.m.s.d. angles (°)	1.19	1.33
Ramachandran plot		
Favourable	94.7%	88.5%
Additional	5.3%	11.0%
Generous	0.0%	0.3%
Disallowed	0.0%	0.3% (Asp-50)

<b>, mean atomic B-factor.

regions involved in ATP binding are not fully ordered (see above; Table I; Figure 2A).

As predicted from sequence alignments (Markus *et al*., 1998; Aravind and Koonin, 1999), the eubacterial C-terminal domain of TyrRS has a core fold with a similar topology to the C-terminal domain of ribosomal protein S4, with a short helical hairpin packed on a mixed β-sheet (see Figure 1 for secondary structure assignment). This structural motif has also been found in *E.coli* Hsp15, which binds the ribosome, and is denoted the αL motif (Staker *et al*., 2000). Using DALI (Holm and Sander, 1993), Hsp15 superposes with a Z-score of 6.7 (61 residues matched, 13 identities, r.m.s.d. on Cα positions of 1.74 Å) and S4 with a Z-score of 5.9 (57 residues matched, 10 identities, r.m.s.d. 1.47 Å). S4, however, differs in having a long insertion of 27 residues between the last two β-strands (Davies *et al*., 1998; Markus *et al*., 1998). The structure of the C-terminal domain of *B.stearothermophilus* TyrRS has recently been determined using NMR (Guijarro *et al*., 2002), and was found to have a very similar structure to that described here.

Crystal structure of the TyrRSTT–tRNA^{tyr} complex

Overall structure. Five different crystal forms of the complex between TyrRSTT and native or transcript tRNA^{tyr} have been analysed, three in which the monomer is in the asymmetric unit and two with the dimer in the asymmetric unit. In all crystal forms, there are two tRNA^{tyr}s bound to each dimer in an essentially symmetrical fashion (Figure 2B), although previous experiments have suggested that TyrRS can only bind one tRNA per dimer (Dessen *et al*., 1982; Bedouelle, 1990). Importantly, co-crystals have only been obtained in the presence of small substrates either with ATP and tyrosinol, or the sulfamoyl analogue of tyrosyl-adenylate or pyrophosphate and tyrosyl-adenylate. The presence of these small substrates leads to a fully ordered, closed active site conformation of the enzyme in which the KMSKS loop interacts with the adenosine base (and triphosphate of ATP if present), as observed in other class I systems in the presence of ATP or adenylate such as GlnRS (Perona *et al*., 1993), TrpRS (Doublie *et al*., 1995) and LeuRS (Cusack *et al*., 2000). This contrasts with the previous reported

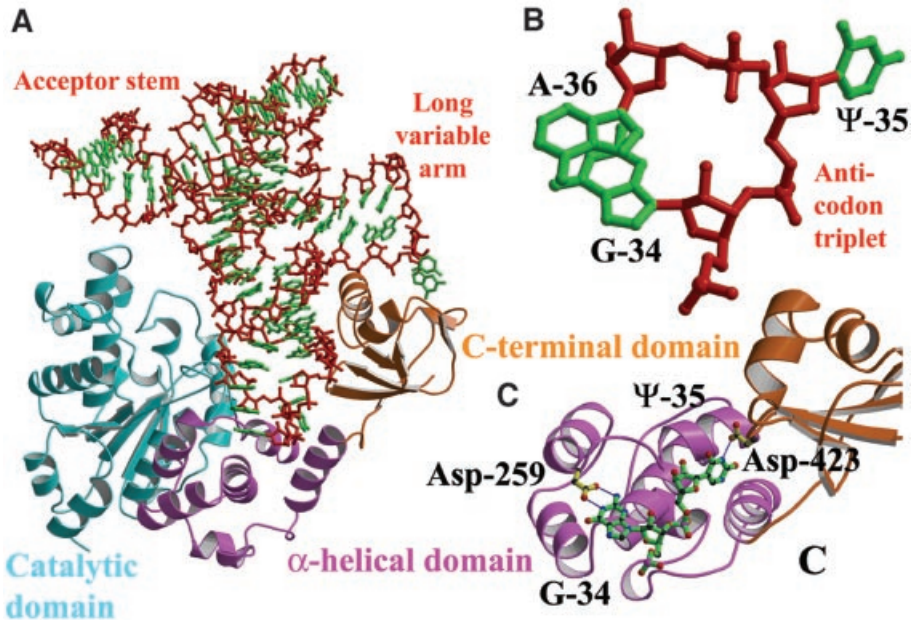

Fig. 3. Interactions between tyrosyl-tRNA synthetase and tRNA^{tyr}. (**A**) The C-terminal domain (orange) binds in the elbow between the long variable arm and the anti-codon stem of the tRNA (red backbone, green bases). The anti-codon stem loop interacts with both the C-terminal domain and the α-helical domain (pink). The tRNA makes no contact with the catalytic domain of the same subunit (cyan). (**B**) The unusual conformation of the anti-codon triplet in which Ade-36 is stacked on Gua-34, while Psu-35 bulges out. (**C**) Base-specific interactions of Asp-259 from the α-helical domain with Gua-34 and Asp-423 from the C-terminal domain with Psu-35.

structures of TyrRSBst in which the KMSKS loop is withdrawn some distance from the active site, in a presumably non-functional conformation, even in the presence of tyrosyl-adenylate (Brick *et al*., 1989). However, in none of our TyrRS–tRNA^{tyr} complex structures is the tRNA 3′-end, beyond the phosphate of C-74, ordered and entering the active site. Nevertheless, the orientation and mode of binding of the tRNA to TyrRSTT, with the tRNA straddling both subunits, are remarkably similar, down to the level of some individual interactions, to the earlier model of the TyrRS–tRNA^{tyr} complex proposed by Labouze and Bedouelle (1989) on the basis of extensive mutational, kinetic and biochemical studies. This correspondence strongly suggests that we have crystallized a functionally important state of the complex that also occurs in solution, if not a state active for aminoacylation. The apparent discrepancy between our symmetrical complexes with two tRNAs bound and the previously reported half-of-the-sites activity of TyrRS both for tyrosine activation (Fersht, 1987) and tRNA binding (Bedouelle, 1990) will be discussed in the conclusion.

The structure we describe at 2.9 Å resolution is that of the complex of TyrRSTT with native tRNA^{tyr}(GΨA) (Egorova *et al*., 1998), in which ATP and tyrosinol are bound in the active site. Crystallographic data from this crystal form, in which the molecular dimer axis coincides with a crystallographic 2-fold axis (and hence the TyrRS dimer is perfectly symmetrical), are given in Table I.

Role of the C-terminal domain in tRNA recognition. The C-terminal domain of TyrRSTT has a crucial role in the recognition of tRNA^{tyr}, first by recognizing the tRNA's unique shape, and secondly by participating in specific interactions with one of the anticodon bases. In the complex with cognate tRNA, the domain is stabilized in a fixed orientation by binding in the elbow between the long variable arm and the anti-codon stem, and the linker peptide connecting it to the last helix of the α-helical domain becomes ordered (Figure 3A). Other than these conformational changes, which are crucial for tRNA binding and recognition, there are no major changes in the backbone conformation of any of the domains of the enzyme upon tRNA binding, although some tRNA interacting side chains (e.g. Lys-251, Arg-255 and Arg-388) are re-orientated. Superposing 73 Cα positions (residues 358–430) from the bound and unbound C-terminal domains from the two structures reported here gives an r.m.s.d. of 0.53 or 0.62 Å (for the A and B chains of the uncomplexed structure, respectively). Similarly, superposing 340 Cα positions (residues 5–344) from the catalytic and α-helical domains of the ternary complex with ATP and tyrosinol (our unpublished data) onto the quaternary complex with tRNA gives an r.m.s.d. of 0.52 Å.

The elements of the C-terminal domain that contact the tRNA are limited largely to the helical hairpin (371–393), which contacts the long variable arm (nucleotides 46–472), and the β hairpin (420–423, notably Arg-420), which contacts the anti-codon stem (nucleotides 28–30) and anticodon (see below). The regions of the tRNA contacted agree very well with protection studies on the *T.thermophilus* system using ethyl-nitrosourea (Egorova *et al*., 1998) and correspond with the two C-terminal clusters of conserved basic residues identified as being in contact with the bound tRNA in the *B.stearothermophilus* system (Bedouelle, 1990; Nair *et al*., 1997). There are hydrogen bond interactions between C-terminal domain residues Trp-370, Arg-373 and Gln-409 and the bases of Gua-471 and Uri-472 in the long variable arm loop, but

these are likely to be characteristic of the *T.thermophilus* system, as these residues and bases are not, in general, conserved. We note that the flexible connection of the tRNA-binding, C-terminal domain of bacterial type TyrRS may have been important in permitting the adaptation of certain mitochondrial TyrRSs to become cofactors in group I intron splicing (Myers *et al*., 2002).

Conformation and recognition of the tRNA^{tyr} anticodon. In the complex, the anticodon triplet of tRNA^{tyr}(GΨA) takes up a novel conformation, in which Gua-34 and Ade-36 are stacked on top of each other and in which Psu-35 bulges out in the opposite direction (Figure 3B). This conformation is stabilized by the maintenance of the usual hydrogen bond between N3 of Uri-33 and the phosphate of Ade-36, and consecutive base stacking of purines 34, 36–38 (see Figure 7). There is base-specific recognition of Psu-35 by Asp-423 (on the last β-hairpin of the C-terminal domain), which hydrogen bonds to the N3 position, and also a hydrogen bond between the main-chain carbonyl of Tyr-342 and the N1 of the base, an interaction specific for pseudouridine (Figure 3C). Although the interactions made by Asp-423 would seem to be important, it is not a phylogenetically conserved residue. Tyr-342, on the last helix of the α-helical domain preceding the linker peptide, partially stacks with Psu-35 (Figure 7). An aromatic residue is generally conserved at this position in the TyrRS in members of the same phylogenetic branch as *T.thermophilus* (e.g. *D.radiodurans*, *A.aeolicus*, *H.influenzae* and *H.pylori*). Interestingly, it has recently been shown biochemically that in the *B.stearothermophilus* TyrRS system, another residue, Phe-323, also in the last helix of the α-helical domain and conserved in most TyrRSs, provides an essential aromatic function for tRNA^{tyr} recognition (Gaillard and Bedouelle, 2001). However, Phe-323 in TyrRSBSt structurally aligns with Ala-346 in TyrRSTT (Figure 1), suggesting that the exact roles of aromatic residues at these distinct positions are different. In most TyrRSs, in members of the same phylogenetic branch as *T.thermophilus* (but not TyrRSTT itself), there is a conserved aromatic residue at both positions (see alignment in figure 2 of Gaillard and Bedouelle, 2001). Base-specific interactions also occur between the N1 and N2 positions of Gua-34 and the carboxyl group of Asp-259. This residue is conserved as a glutamate or aspartate in all known bacterial and mitochondrial TyrRSs, although it is not conserved in archaeal and eukaryotic sequences, which have a weaker interaction with the anti-codon bases (Fechter *et al*., 2001). In the same loop between two helices in the α-helical domain, Arg-256 closely contacts the backbone of Psu-35. The base Ade-36 makes no specific interactions, but makes van der Waal's contact with the protein in the region of Pro-285 on its face opposite to that stacking with Gua-34.

Relatively few systematic experiments have been carried out on the identity elements of bacterial tRNA^{tyr}, but the above observations on the *T.thermophilus* system are consistent with available results in other systems. The comparative study of phosphate protection upon tRNA binding to the synthetase in the *T.thermophilus* and *E.coli* systems shows that the mode of tRNA binding is very similar (Egorova *et al*., 1998). In the *E.coli* system, the change Gua-34→Cyt causes a 24-fold decrease in the catalytic efficiency of aminoacylation (Hou and Schimmel, 1989), and changing Uri-35→Gua causes a 200-fold decrease (Himeno *et al*., 1990). Thus, the anticodon bases 34–35 are shown both biochemically and structurally to be important recognition elements by the synthetase.

Conformation of the long variable arm of tRNA^{tyr} compared with that of tRNA^{ser}. It has been proposed that a key determinant in the orientation of the long variable arm of class 2 tRNAs is the number of unpaired nucleotides at the 3′-end of the long variable arm. In the case of tRNA^{tyr}, this is of critical importance as a positive identity element for recognition by TyrRS and as a negative identity element preventing mischarging of tRNA^{tyr} by LeuRS and SerRS, which also have long variable arm cognate tRNAs (Himeno *et al*., 1990; Asahara *et al*., 1993). The two key differences in the secondary structures of tRNA^{tyr} and tRNA^{ser} are: (i) that they have, respectively, a phylogenetically conserved adenosine or guanosine at position 20B in the D-loop; and (ii) that tRNA^{tyr} has two unpaired uridines (U48-1 and U48-2) at the base of the long variable arm preceding nucleotide 48, whereas tRNA^{ser} has no unpaired bases at this position (Figure 4A). Elimination of the two unpaired uracils at the 3′ base of the variable arm in *E.coli* tRNA^{tyr} leads to a 150-fold decrease in tyrosylation efficiency (Himeno *et al*., 1990).

The current structure and its comparison with the corresponding *T.thermophilus* seryl-tRNA synthetase–tRNA^{ser} complex (Biou *et al*., 1994), the only two crystal structures of long variable arm tRNAs, now permits us to examine this hypothesis further. In both tRNAs, the D-loop has the same number of nucleotides and a similar conformation to nucleotide 20A, forming a planar base-triple with the Levitt pair (G15–C48) and with the base 20B inserted into the tRNA core. This makes the backbone conformation of the two tRNAs, apart from the variable loop, rather similar (46 phosphates can be superimposed with an r.m.s.d. of 1.16 Å). However, the details of the core packing are significantly different (Figure 4B), resulting in an ~50° change in orientation of the long variable arm helix (Figure 4C), which clearly permits shape discrimination between these two class 2 tRNAs by their respective synthetases. In tRNA^{ser}, the significant tilt of bases Ade-21 and Gua-9 (which stack in a parallel manner) allows deep penetration of Gua-20B into the core to stack against the first base pair of the long variable arm (A45–U48-1). In contrast, in tRNA^{tyr}, the first base pair of the long variable is formed by a reverse Hoogsteen base pair between Ade-20B and Uri-48-2, against which the unpaired Uri-48-1 stacks. Ade-20B penetrates less far into the tRNA core, perhaps excluded by Ade-21, which forms a much more planar base-triple with Uri-8 and Ade-14 than in tRNA^{ser}. The N6 of Ade-21 also forms a single hydrogen bond to the O2 of Uri-48-1, helping to maintain this planarity and to position the latter. In tRNA^{tyr}, the orientation of base Ade-21 is no longer strongly coupled to that of nucleotide 9, in contrast to the situation in tRNA^{ser}, where the strong stacking of Gua-9 on Ade-14 ensures that both bases remain markedly tilted (see Figure 4B). The lack of stacking, in turn, may be due to the presence of the pyrimidine Uri-9 in tRNA^{tyr}, which has been noted by

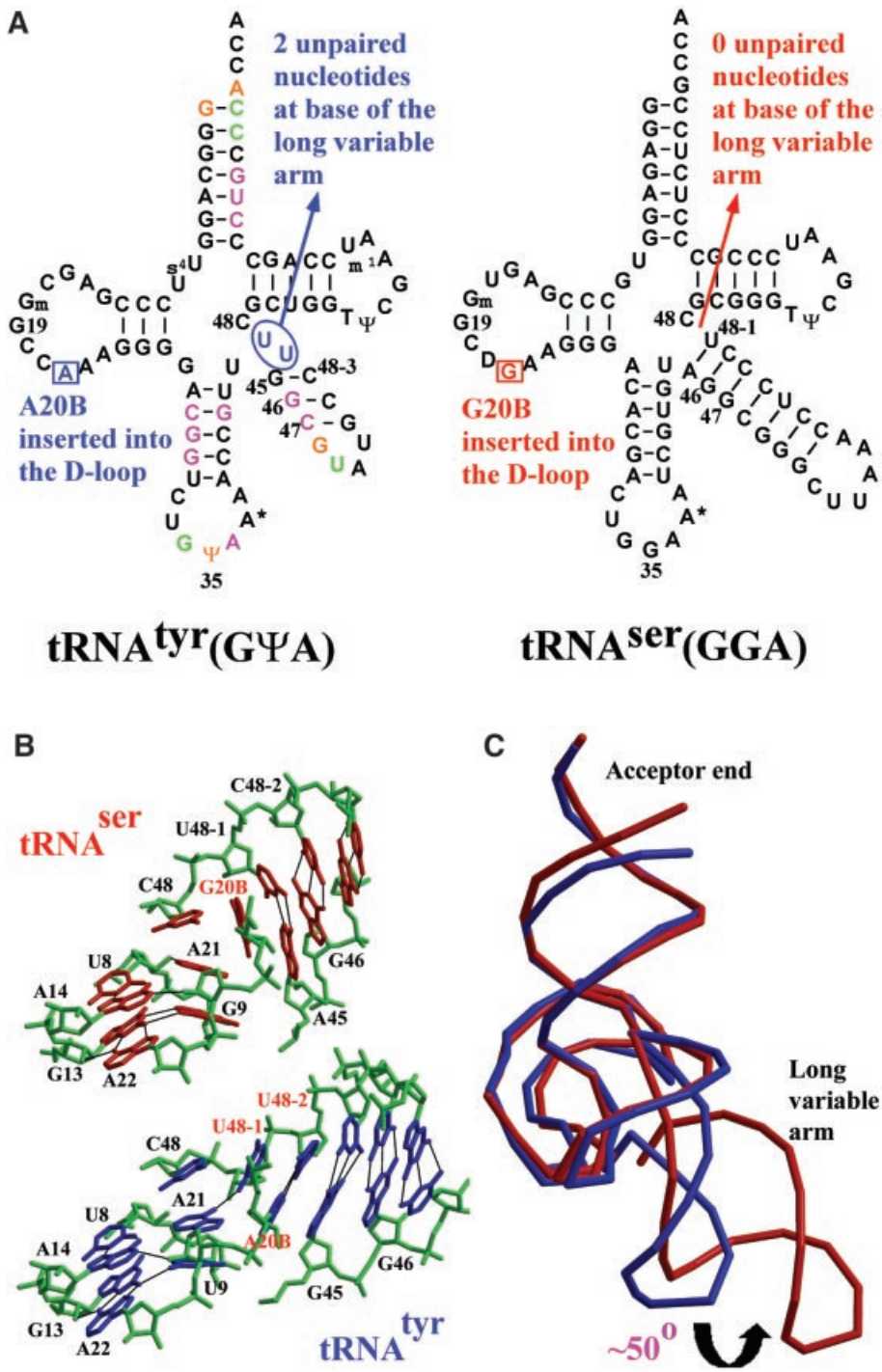

Fig. 4. Structure of tRNAtyr compared with that of tRNA^{ser}. (**A**) Comparison of the secondary structures of *T.thermophilus* tRNA^{tyr}(GΨA) (left) and tRNA^{tyr}(GGA) (right), highlighting differences, conserved in other prokaryotic organisms, that determine the orientation of the long variable arm. tRNA^{tyr} nucleotides with only backbone contacts to TyrRSTT are shown in purple, those with only base contacts are shown in green and those with backbone and base contacts are shown in orange. (**B**) Comparison of the 3D structures of the base of the long variable arm in *T.thermophilus* tRNA^{tyr} and *T.thermophilus* tRNA^{ser} (Biou *et al*., 1994), based on the structural alignment in (C). In tRNA^{ser}, Gua-20B is unpaired and stacks against the first base pair of the long variable arm, which comprises A45:U48-1 (top). In tRNA^{tyr}, U48-1 is unpaired and stacks against the first base pair of the long variable arm, which comprises A20B:U48–2 (bottom). (**C**) View looking down the anticodon stem-loop of the structural alignment of tRNA^{tyr} (blue) and tRNA^{ser} (red) based on superposition of 46 phosphates from the acceptor stem, D- and T-loops (r.m.s.d. = 1.16 Å). The tRNA cores have a very similar structure, but the variable arms project at an angle differing by ~50°.

Nissan *et al*. (1999) and Nissan and Perona (2000) to be rather unusual in class 2 tRNAs and correlates with the occurrence of 3′ unpaired nucleotides in the variable stem, as in this case. In tRNA^{tyr}, the base of Uri-9 makes a weak triple (one hydrogen bond) with Gua-13 and Ade-22, whereas in tRNA^{ser}, the base of Gua-9 makes two hydrogen bonds with Gua-13 and Ade-22, although in both cases the base of nucleotide 9 is tilted. A further

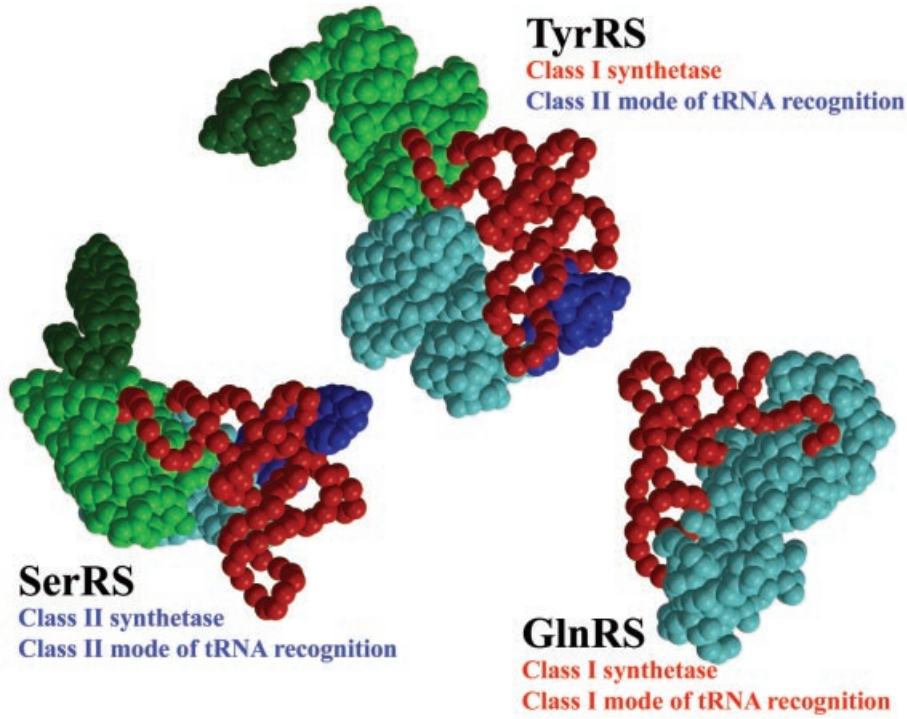

Fig. 5. Schematic diagrams showing different modes of tRNA recognition by TyrRS, SerRS and GlnRS. TyrRS (class I) and SerRS (class 2) both have a class II mode of tRNA recognition approaching the tRNA acceptor stem from the major groove side. GlnRS has a canonical class I mode of tRNA recognition approaching the tRNA acceptor stem from the minor groove side. Notably, both SerRS and TyrRS have long variable arm (class 2) tRNAs, are dimeric and have cross-subunit tRNA binding.

correlation noted by Nissan and Perona (2000) is that $tRNA^{tyr}$, with a pyrimidine at position 9, also conserves a C at position 20A. The base of 20A forms a triple with the reverse Watson–Crick G15–C48 (Levitt) base pair in both $tRNA^{ser}$ and $tRNA^{tyr}$, with the necessary slight shift in position to maintain two hydrogen bonds with G15 of either dihydrouridine-20A ($tRNA^{ser}$) or Cyt-20A ($tRNA^{tyr}$). Further mutational studies, along the lines of the careful work of Nissan *et al*. (1999) and Nissan and Perona (2000), would be required to assess the relative importance of all these factors for determining the tRNA stability and variable arm orientation, although it is likely that the presence of Ade-20B and two 3′-unpaired uracils in the variable arm are the key features.

Acceptor stem recognition. The acceptor stem of the tRNA binds across the dimer interface onto the catalytic domain of the opposing subunit (Figure 2B). Two regions of this domain make important contacts: (i) residues 148–154, in particular Thr-148, Gln-151 and Glu-154, which partially overlap with the dimer interface; and (ii) the helix α11 formed by residues 198–211, in particular Arg-198 (Trp-196 in TyrRSBst; Figure 1), Leu-202, Arg-205, Glu-206 and Arg-209 (Arg-207 in TyrRSBst). These regions correspond to clusters 1 and 2, which were previously identified as contacting the tRNA (Bedouelle, 1990; Nair *et al*., 1997). Residues 21–27 also play an important secondary role in positioning side chains of directly interacting residues, notably Arg-198 and Arg-205, and in addition Val-23 (Thr-17 in TyrRSBst) packs against the ribose of Gua-1. Direct interactions are made to the tRNA backbone of nucleotides 67–69 on the 3′-strand and the 5′-phosphate of Gua-1 (Arg-205, Arg-209) as well as base-specific interactions in the major groove with Cyt-71 (Glu-154), Cyt-72 (Glu-154) and Ade-73 (Arg-198, Glu-154). Leu-202 packs on the base of Gua-1. Specific recognition of the discriminator base Ade-73 is made through a hydrogen bond between the N6 position and the main-chain carbonyl oxygen of Glu-154, an interaction that was predicted in the model for the *B.stearothermophilus* complex where Ala-150 is the equivalent residue (Labouze and Bedouelle, 1989). In addition, Arg-198 hydrogen bonds to the N3 position of Ade-73. These interactions give a rationale for the strong preference for adenosine as the discriminator base, with any other nucleotide reducing the catalytic efficiency by factors from 38 (A→G) to 8 (A→C) (Himeno *et al*., 1990) and causing loss of *in vivo* tyrosine specificity (Sherman *et al*., 1992). The interactions of Glu-154 with the N4 positions of Cyt-71 and Cyt-72, and Arg-198 with the N3 of Gua-1, also rationalize the phylogenetic preference of G–C as the first base pair in bacterial $tRNA^{tyr}$, although it is not a strong identity element. Finally, the structure supports the important, but purely negative, discriminatory role proposed for Glu-152 in TyrRSBst, which helps reject non-cognate tRNAs by an electrostatic mechanism (Bedouelle and Nageotte, 1995); the equivalent residue in TyrRSTT is Glu-156, which is very close but does not touch the tRNA acceptor stem directly.

Conclusion

Extensive functional studies on wild-type and mutant TyrRSBSt by Ferhst and co-workers have characterized tyrosyl-tRNA synthetase as an intrinsically asymmetric homodimer with half of the site's enzymatic activity (Fersht, 1987; Ward and Fersht, 1988a,b). In addition,

various studies have shown that the TyrRSBSt or TyrRSEC dimer can only bind one tRNA in solution (Dessen *et al*., 1982; Bedouelle, 1990). In view of these results, it would seem contradictory to observe, as presented here, a perfectly symmetrical TyrRSTT–tRNA^{tyr}–ATP–tyrosinol complex, and it raises questions about the functional significance of the structure. However, this is not a new problem, as many crystal structures of TyrRS, whether native or with small substrates, are either nearly (if the dimer is in the asymmetric unit) or perfectly symmetrical (Brick and Blow, 1987; Brick *et al*., 1989; our unpublished results) and the discrepancy has been discussed previously in the literature (e.g. Ward and Fersht, 1988a). Our understanding of this situation is the following. Careful reading of the literature of Fersht's group shows that whereas the TyrRS enzyme exhibits strong negative co-operativity such that on short time scales tyrosyl-adenylate is only formed in one active site, on a longer time scale, tyrosyl-adenylate is formed in the second active site, converting the enzyme again to a symmetrical form. The half-life of formation of the first tyrosyl-adenylate is 39 ms (k = 17.8/s) and for the second it is 3.8 min (k = 0.003/s) for the case of TyrRSBSt (Mulvey and Fersht, 1977). Clearly, in a crystallization experiment, there is ample time for substrate binding to both active sites and there is quite likely preferential crystallization of a symmetrical form, as is frequently observed. In the case of tRNA binding, we believe the same arguments hold. In all our crystal forms of the complex, there are small substrates (ATP + tyrosinol or tyrosyl-adenylate) bound in both active sites, making a symmetrical dimer to which there is clearly no steric hinderance for binding of two tRNA molecules. However, it may require an asymmetric form of the dimer with one bound tRNA, a form we have not yet managed to crystallize, to observe the 3′ end of the tRNA functionally bound in the active site. We note that the small angle neutron scattering experiments of Dessen *et al*. (1982), which showed only one tRNA binding the dimer, were performed with no small substrates present. It would clearly be interesting to repeat these experiments in the presence of small substrates, corresponding to the crystallization conditions of the complex.

Despite having an unambiguous class I catalytic domain, tyrosyl-tRNA synthetase is in two important ways a non-canonical class I synthetase, as deduced previously from biochemical studies (Bedouelle *et al*., 1993) and visualized explicitly in the current structure. First, it is a functional dimer with cross-subunit tRNA binding (Figure 2B), a feature shared in class I synthetases only with its subclass Ic partner, tryptophanyl-tRNA synthetase. Secondly, it has a class II mode of tRNA recognition (Figure 5). This means that it interacts with tRNA^{tyr} from the variable loop and acceptor stem major groove side as, for instance, in the case of class II AspRS (Ruff *et al*., 1991) and SerRS (Cusack *et al*., 1996), without requiring distortion of the 3′ end of the tRNA from its helical path to enter the active site. This is in strong contrast to canonical class I systems such as those of subclass Ib GlnRS (Rould *et al*., 1989; Rath *et al*., 1998) and subclass Ia ArgRS (Delagoutte *et al*., 2000), which approach cognate tRNA from the acceptor stem minor groove side and require a hairpin distortion of the tRNA 3′-end so that they can enter the active site. Despite this class II mode of tRNA recognition, TyrRS preferentially aminoacylates the 2′ OH of Ade-76 in accordance with other class I systems, although it can also apparently aminoacylate the 3′ OH (Cramer *et al*., 1975). The evolutionary scenario that led to these non-canonical features of TyrRS is not obvious, although the pairing of TyrRS and the class II synthetase PheRS (which anomalously aminoacylates at the 2′OH position) in a new hypothesis about the origin of the two synthetase classes is intriguing in this respect (Ribas de Pouplana and Schimmel, 2001). However, superposition of the GlnRS–tRNA^{gln} or ArgRS–tRNA^{arg} complex on TyrRS by means of the conserved Rossmann fold shows that the normal hairpin mode of class I tRNA binding is incompatible with dimerization of TyrRSTT (Figure 6). On the other hand, the observed class II mode of recognition of TyrRS for tRNA^{tyr}, modelled to extend into the active site according to the model of Labouze and Bedouelle (1989), is clearly

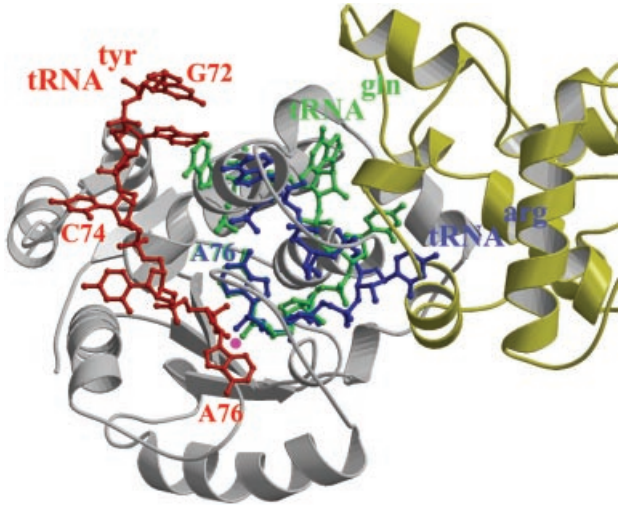

Fig. 6. Model of the 3′ CCA end of tRNA^{tyr} in the active site of TyrRSTT. The C74-C75-A76 3′ extremity of tRNA^{tyr} (red) is modelled in the active site of TyrRSTT by matching the predicted model of Labouze and Bedouelle (1989) to the experimental structure (this work) of tRNA^{tyr}, which extends only to A73. Due to the close agreement of the position of the tRNA^{tyr} in the experimental and predicted models, this is possible with only minor adjustments to avoid steric clashes with enzyme side-chains. The backbone conformation of the CCA and the positions of the bases are by no means necessarily correct. The aim is to show that the observed class II mode of tRNA binding to TyrRSTT is compatible with unhindered entry of the 3′ end into the active site without major conformational changes (although it cannot be excluded that these occur), allowing the positioning of the 2′ OH of the terminal ribose (marked with a purple spot) adjacent to the carboxyl group of the substrate amino acid (not shown for clarity, since it is underneath in this view). This is clearly not the case for a class I mode of entry into the active site as exemplified by tRNA^{arg} (blue) or tRNA^{gln} (green). These tRNA 3′ ends were drawn after superposition of the Rossmann fold of TyrRSTT with that of yeast ArgRS (Delagoutte *et al*., 2000) or *E.coli* GlnRS (Rath *et al*., 1998) in the context of their respective tRNA complexes. Note that the bases of C75 in tRNA^{arg}, and G73 and C75 in tRNA^{gln} have been omitted for clarity. Although the 3′ hairpin conformations of tRNA^{arg} and tRNA^{gln}, from subclasses Ia and Ib, respectively, are somewhat different, the base of A76 and the position of the 2′ OH (purple spot) superpose very closely. It is clear that the CCA ends of these two class I mode tRNAs would both clash irremediably with the dimer interface of TyrRS (one subunit is grey, the other yellow), and A76 and C75 coincide with the position of the important active site loop residues 83–86 in TyrRS.

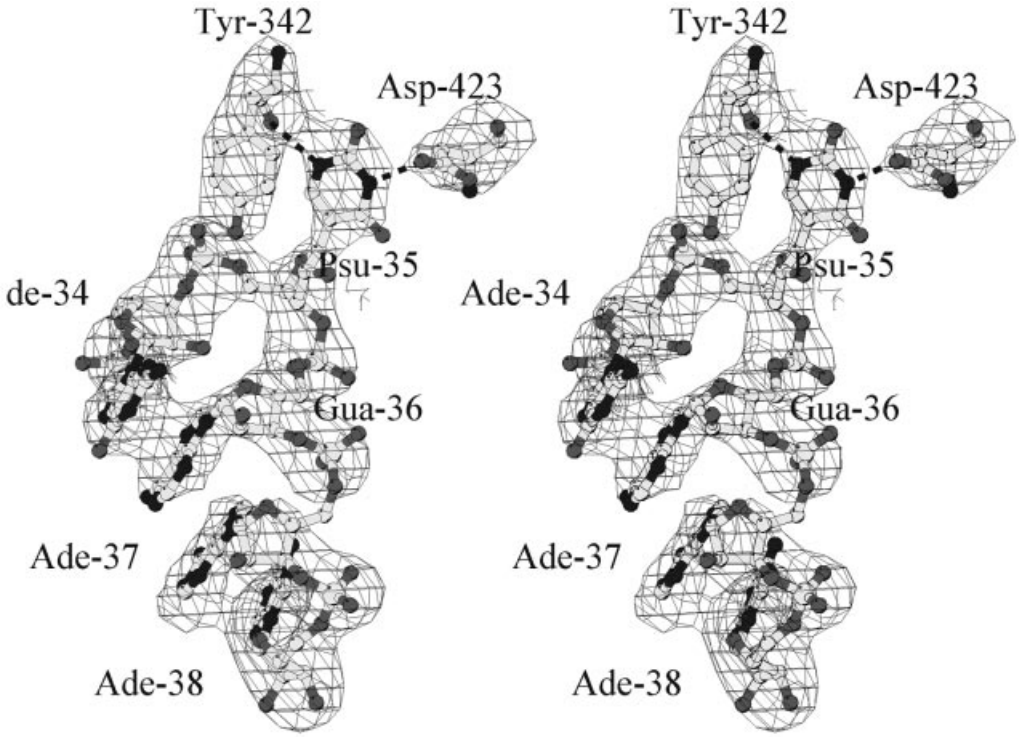

Fig. 7. Simulated omit map showing electron density for the tRNA^{tyr} anticodon loop. Stereoview showing electron density for the anticodon loop bases 34–38 and residues Tyr-342 and Asp-423, which hydrogen bond (dashed lines) to base Ψ-35. Note that purines Ade-34, Gua-36, Ade-37 and Ade-38 are stacked on top of each other. The map is a simulated annealing difference map, calculated using a standard CNS protocol and contoured at 2σ (Brünger *et al*., 1998).

compatible with dimerization, at the same time as allowing the 2′ OH of the terminal ribose to be correctly positioned for aminoacylation (Figure 6). This suggests that dimerization and the class II mode of tRNA recognition in TyrRS may be evolutionarily linked, in that one may have necessitated the other. A crystal structure of the TyrRS–tRNA^{tyr} complex, active for aminoacylation and perhaps necessarily asymmetric, is clearly required to give further insight into this still puzzling enigma.

Very recently, we have determined a crystal structure at 1.95 Å resolution of a complex of TyrRSTT with a tRNA^{tyr} transcript in the absence of small substrates. This new high resolution structure confirms the conclusions described here and shows more clearly the entry of the 3′ end of the tRNA into the active site, which is in an open conformation. The complex is crystallographically symmetrical with two tRNAs per tyrosyl-tRNA synthetase dimer.

Materials and methods

The gene for *T.thermophilus* (strain HB27) TyrRS was cloned and sequenced, and found to code for a protein subunit of 432 residues (A.Yaremchuk, S.Cusack and M.Tukalo, unpublished results). Overproduction and purification of TyrRSTT were carried out in a similar way to that of the *T.thermophilus* LeuRS (Yaremchuk *et al*., 2000). *Thermus thermophilus* tRNA^{tyr}(GΨA) was purified from strain HB-27 as described previously (Egorova *et al*., 1998). Crystals of TyrRS alone and in complex with tyrosinol were obtained by the hanging drop vapour diffusion technique using equal volumes of the protein (12 mg/ml) and a reservoir solution that contained 1.2 M ammonium sulfate, 10 mM $MgCl_2$, 0.5 mM dithiothreitol (DTT) and 50 mM MES pH 5.8. Crystals of TyrRS in complex with tyrosinol, ATP and tRNA^{tyr} were grown at 293 K by the equilibration of 4 µl of protein/tRNA solution (4–5 mg/ml of TyrRSTT, molar ratio of protein:tRNA of 1:1 or 1:2.2, 5 mM tyrosinol, 10 mM $MgCl_2$, 10 mM ATP, 50 mM HEPES pH 7.0 and 0.8 M ammonium sulfate) against 1 ml of reservoir solution containing 1.5–1.6 M ammonium sulfate and 100 mM HEPES pH 7.0. Hexagonal bipyramid crystals grew to final dimensions of up to 500 µm within 2–4 weeks, depending on the protein/tRNA molar ratio.

Crystallography

Data collection statistics are given in Table I. Data were integrated with MOSFLM (Leslie, 1999) and subsequent processing was carried out using the CCP4 package (CCP4, 1994). Both structures were solved by molecular replacement using MOLREP. The search model employed was that of the catalytic and α-helical domain of TyrRSTT determined previously *de novo* at 2.1 Å resolution in a different crystal form (A.Yaremchuk, M.Tukalo and S.Cusack, unpublished results). For the 2.0 Å resolution structure of the complete enzyme, the ARP/wARP program (Perrakis *et al*., 1999) was used to automatically build the additional C-terminal domains and to add water molecules. Both structures were refined using CNS (Brünger *et al*., 1998). Due to the moderate resolution and high B-factors of the tRNA, base planarity, base pair and ribose pucker restraints were applied. Ribose puckers of nucleotides 7, 9, 18–20, 202 (20B), 34–35, 48, 58 and 60 were restrained to C2′ endo, and all others to C3′ endo. The refinement statistics and quality of structures are given in Table I. A simulated omit map of a portion of the tRNA electron density in the region of the anti-codon loop is shown in Figure 7.

Figures 2–5 were prepared with BOBSCRIPT (Esnouf, 1999) and rendered with RASTER3D (Merritt and Bacon, 1997).

Acknowledgements

The authors thank members of the ESRF-EMBL Joint Structural Biology Group for access to ESRF beamlines. This work was supported in part by an International Research Scholar's award from the Howard Hughes Medical Institute (to M.T.), and in part by Human Frontiers Science Programme Research grant RGP0190/2001-M.

References

Aravind,L. and Koonin,E.V. (1999) Novel predicted RNA-binding domains associated with the translation machinery. *J. Mol. Evol.*, **48**, 291–302.

Asahara,H., Himeno,H., Tamura,K., Hasegawa,T., Watanabe,K. and Shimizu,M. (1993) Recognition nucleotides of *Escherichia coli* tRNA^{Leu} and its elements facilitating discrimination from tRNA^{Ser} and tRNA^{Tyr}. *J. Mol. Biol.*, **231**, 219–229.

Bedouelle,H. (1990) Recognition of tRNA^{tyr} by tyrosyl-tRNA synthetase. *Biochimie*, **72**, 589–598.

Bedouelle,H. and Nageotte,R. (1995) Macromolecular recognition through electrostatic repulsion. *EMBO J.*, **14**, 2945–2950.

Bedouelle,H., Guez-Ivanier,V. and Nageotte,R. (1993) Discrimination between transfer-RNAs by tyrosyl-tRNA synthetase. *Biochimie*, **75**, 1099–1108.

Bhat,T.N., Blow,D.M., Brick,P. and Nyborg,J. (1982) Tyrosyl-tRNA synthetase forms a mononucleotide-binding fold. *J. Mol. Biol.*, **158**, 699–709.

Biou,V., Yaremchuk,A., Tukalo,M.A. and Cusack,S. (1994) The 2.9Å crystal structure of *T. thermophilus* seryl-tRNA synthetase complexed with tRNA^{ser}. *Science*, **263**, 1404–1410.

Brick,P. and Blow,D.M. (1987) Crystal structure of a deletion mutant of a tyrosyl-tRNA synthetase complexed with tyrosine. *J. Mol. Biol.*, **194**, 287–294.

Brick,P., Bhat,T.N. and Blow,D.M. (1989) Structure of tyrosyl-tRNA synthetase refined at 2.3Å resolution. Interaction of the enzyme with the tyrosyl-adeylate intermediate. *J. Mol. Biol.*, **208**, 83–98.

Brünger,A.T. *et al.* (1998) Crystallographic and NMR system: a new software suite for macromolecular structure determination. *Acta Crystallogr. D*, **54**, 905–921.

CCP4 (1994) The CCP4 suite: programs for protein crystallography. *Acta Crystallogr. D*, **50**, 760–763.

Cramer,F., Faulhammer,H., von der Haar,F., Sprinzl,M. and Sternbach,H. (1975) Aminoacyl-tRNA synthetases from baker's yeast: reacting site of aminoacylation is not uniform for all tRNAs. *FEBS Lett.*, **56**, 212–214.

Cusack,S. (1995) Eleven down and nine to go. *Nat. Struct. Biol.*, **2**, 824–831.

Cusack,S., Yaremchuk,A. and Tukalo,M. (1996) The crystal structure of the ternary complex of *T. thermophilus* seryl-tRNA synthetase with tRNA^{ser} and a seryl-adenylate analogue reveals a conformational switch in the active site. *EMBO J.*, **15**, 2834–2842.

Cusack,S., Yaremchuk,A. and Tukalo,M. (2000) The 2Å crystal structure of leucyl-tRNA synthetase and its complex with a leucyl-adenylate analogue. *EMBO J.*, **19**, 2351–2361.

Davies,C., Gerstner,R.B., Draper,D.E., Ramakrishnan,V. and White, S.W. (1998) The crystal structure of ribosomal protein S4 reveals a two-domain molecule with an extensive RNA-binding surface: one domain shows structural homology to the ETS DNA-binding motif. *EMBO J.*, **17**, 4545–4558.

Delagoutte,B., Moras,D. and Cavarelli,J. (2000) tRNA aminoacylation by arginyl-tRNA synthetase: induced conformations during substrates binding. *EMBO J.*, **19**, 5599–5610.

Dessen,P., Zaccai,G. and Blanquet,S. (1982) Neutron scattering studies of *Escherichia coli* tyrosyl-tRNA synthetase and of its interaction with tRNA^{tyr}. *J. Mol. Biol.*, **159**, 651–664.

Doublie,S., Bricogne,G., Gilmore,C. and Carter,C.W.,Jr (1995) Tryptophanyl-tRNA synthetase crystal structure reveals an unexpected homology to tyrosyl-tRNA synthetase. *Structure*, **3**, 17–31.

Egorova,S.P., Iaremchuk,A.D., Kriklivyi,I.A. and Tukalo,M.A. (1998) Comparative analysis of interaction sites of *Thermus thermophilus* and *Escherichia coli* tRNA(Tyr) with homologous aminoacyl-tRNA synthetases by means of chemical modification and nuclease hydrolysis. *Russ. J. Bioorg. Chem.*, **24**, 524–530.

Esnouf,R.M. (1999) Further additions to Molscript version 1.4, including reading and contouring of electron density maps. *Acta Crystallogr. D*, **55**, 938–940.

Fechter,P., Rudinger-Thirion,J., Tukalo,M. and Giege,R. (2001) Major tyrosine identity determinants in *Methanococcus jannaschii* and *Saccharomyces cerevisiae* tRNA^{tyr} are conserved but expressed differently. *Eur. J. Biochem.*, **268**, 761–767.

Fersht,A.F. (1987) Dissection of the structure and activity of the tyrosyl-tRNA synthetase by site-directed mutagenesis. *Biochemistry*, **26**, 8031–8037.

First,E.A. (1997) Catalysis of tRNA aminoacylation by class I and II aminoacyl-tRNA synthetases. In Sinnott,M. (ed.), *Comprehensive Biological Catalysis*. Vol. 1. Academic Press, London, UK, pp. 573–607.

Gaillard,C. and Bedouelle,H. (2001) An essential residue in the flexible peptide linking the two idiosyncratic domains of bacterial tyrosyl-tRNA synthetases. *Biochemistry*, **40**, 7192–7199.

Gouet,P., Courcelle,E., Stuart,D.I. and Metoz,F. (1999) ESPript: multiple sequence alignments in PostScript. *Bioinformatics*, **15**, 305–308.

Guez,V., Nair,S., Chaffotte,A. and Bedouelle,H. (2000) The anticodon-binding domain of tyrosyl-tRNA synthetase: state of folding and origin of the crystallographic disorder. *Biochemistry*, **39**, 1739–1747.

Guijarro,J.I., Pintar,A., Prochnicka-Chalufour,A., Guez,V., Gilquin,B., Bedouelle,H. and Delepierre,M. (2002) Structure and dynamics of the anticodon-arm binding domain of *Bacillus stearothermophilus* tyrosyl-tRNA synthetase. *Structure*, **10**, 311–317.

Himeno,H., Hasegawa,T., Ueda,T., Watanabe,K. and Shimizu,M. (1990) Conversion of aminoacylation specificity from tRNA^{Tyr} to tRNA^{Ser} *in vitro*. *Nucleic Acids Res.*, **18**, 6815–6819.

Holm,L. and Sander,C. (1993) Protein structure comparison by alignment of distance matrices. *J. Mol. Biol.*, **233**, 123–138.

Hou,Y.M. and Schimmel,P. (1989) Modeling with *in vitro* kinetic parameters for the elaboration of transfer RNA identity *in vivo*. *Biochemistry*, **28**, 4942–4947.

Kabsch,W. and Sander,C. (1983) Dictionary of protein secondary structure: pattern recognition of hydrogen-bonded and geometrical features. *Biopolymers*, **22**, 2577–2637.

Labouze,E. and Bedouelle,H. (1989) Structural and kinetic bases for the recognition of tRNA^{Tyr} by tyrosyl-tRNA synthetase. *J. Mol. Biol.*, **205**, 729–735.

Leslie,A.G. (1999) Integration of macromolecular diffraction data. *Acta Crystallogr. D*, **55**, 1696–1702.

Markus,M.A., Gerstner,R.B., Draper,D.E. and Torchia,D.A. (1998) The solution structure of ribosomal protein S4 Δ41 reveals two subdomains and a positively charged surface that may interact with RNA. *EMBO J.*, **17**, 4559–4571.

Merritt,M.A. and Bacon,D.J. (1997) Raster 3D: photorealistic molecular graphics. *Methods Enzymol.*, **277**, 505–524.

Mulvey,R.S. and Fersht,A.R. (1977) Ligand binding stoichiometries, subunit structure and slow transitions in aminoacyl-tRNA synthetases. *Biochemistry*, **16**, 4005–4013.

Myers,C.A., Kuhla,B., Cusack,S. and Lambowitz,A.M. (2002) tRNA-like recognition of group I introns by a tyrosyl-tRNA synthetase. *Proc. Natl Acad. Sci. USA*, **99**, 2630–2635.

Nair,S., Ribas de Pouplana,L., Houman,F., Avruch,A., Shen,X. and Schimmel,P. (1997) Species-specific tRNA recognition in relation to tRNA synthetase contact residues. *J. Mol. Biol.*, **269**, 1–9.

Nissan,T.A. and Perona,J.J. (2000) Alternative designs for construction of the class II transfer RNA tertiary core. *RNA*, **6**, 1585–1596.

Nissan,T.A., Oliphant,B. and Perona,J.J. (1999) An engineered class I transfer RNA with a class II tertiary fold. *RNA*, **5**, 434–445.

Perona,J.J., Rould,M.A. and Steitz,T.A. (1993) Structural basis for transfer RNA aminoacylation by *Escherichia coli* glutaminyl-tRNA synthetase. *Biochemistry*, **32**, 8758–8771.

Perrakis,A., Morris,R. and Lamzin,V.S. (1999) Automated protein model building combined with iterative structure refinement. *Nat. Struct. Biol.*, **6**, 458–463.

Qiu,X. *et al*. (2001) Crystal structure of *Staphylococcus aureus* tyrosyl-tRNA synthetase in complex with a class of potent and specific inhibitors. *Protein Sci.*, **10**, 2008–2016.

Quinn,C.L., Tao,N. and Schimmel,P. (1995) Species-specific microhelix aminoacylation by a eukaryotic pathogen tRNA synthetase dependent on a single base-pair. *Biochemistry*, **34**, 12489–12495.

Rath,V.L., Silvian,L.F., Beijer,B., Sproat,B.S. and Steitz,T.A. (1998) How glutaminyl-tRNA synthetase selects glutamin. *Structure*, **6**, 439–449.

Ribas de Pouplana,L. and Schimmel,P. (2001) Two classes of tRNA synthetases suggested by sterically compatible dockings on tRNA acceptor stem. *Cell*, **104**, 191–193.

Rould,M.A., Perona,J.J., Söll,D. and Steitz,T.A. (1989) Structure of *E. coli* glutaminyl-tRNA synthetase complexed with tRNA^{Gln} and ATP at 2.8Å resolution. *Science*, **246**, 1135–1142.

Ruff,M., Krishnaswamy,S., Boeglin,M., Poterszman,A., Mitschler,A., Podjarny,A., Rees,B., Thierry,J.C. and Moras,D. (1991) Class II aminoacyl transfer RNA synthetases: crystal structure of yeast aspartyl-tRNA synthetase complexed with tRNA(Asp). *Science*, **252**, 1682–1689.

Sherman,J.M., Rogers,K., Rogers,M.J. and Soll,D. (1992) Synthetase competition and tRNA context determine the *in vivo* identify of tRNA discriminator mutants. *J. Mol. Biol.*, **228**, 1055–1062.

Staker,B.L., Korber,P., Bardwell,J.C. and Saper,M.A. (2000) Structure of Hsp15 reveals a novel RNA-binding motif. *EMBO J.*, **19**, 749–757.

Steer,B.A. and Schimmel,P. (1999) Major anticodon-binding region missing from an archaebacterial tRNA synthetase. *J. Biol. Chem.*, **274**, 35601–35606.

Ward,W.H. and Fersht,A.R. (1988a) Asymmetry of tyrosyl-tRNA synthetase in solution. *Biochemistry*, **27**, 1041–1049.

Ward,W.H. and Fersht,A.R. (1988b) Tyrosyl-tRNA synthetase acts as an asymmetric dimer in charging tRNA. A rationale for half-of-the-sites activity. *Biochemistry*, **27**, 5525–5530.

Wolf,Y.I., Aravind,L., Grishin,N.V. and Koonin,E.V. (1999) Evolution of aminoacyl-tRNA synthetases-analysis of unique domain architectures and phylogenetic trees reveals a complex history of horizontal gene transfer events. *Genome Res.*, **9**, 689–710.

Yaremchuk,A., Cusack,S., Gudzera,O., Grøtli,M. and Tukalo,M. (2000) Crystallization and preliminary crystallographic analysis of *Thermus thermophilus* leucyl-tRNA synthetase and its complexes with leucine and a non-hydrolysable leucine-adenylate analogue. *Acta Crystallogr. D*, **56**, 667–669.

Received March 18, 2002; revised May 16, 2002; accepted May 24, 2002